Electronic Supplementary Material (ESI) for Physical Chemistry Chemical Physics.

Supplementary Information for:

Identification of photofragmentation patterns in trihalide anions by global analysis of vibrational wavepacket dynamics in broadband transient absorption data

Sebastian Schott,[a] Lea Ress,[a] Jan Hrušák,[b] Patrick Nuernberger,[c] and Tobias Brixner*[a]

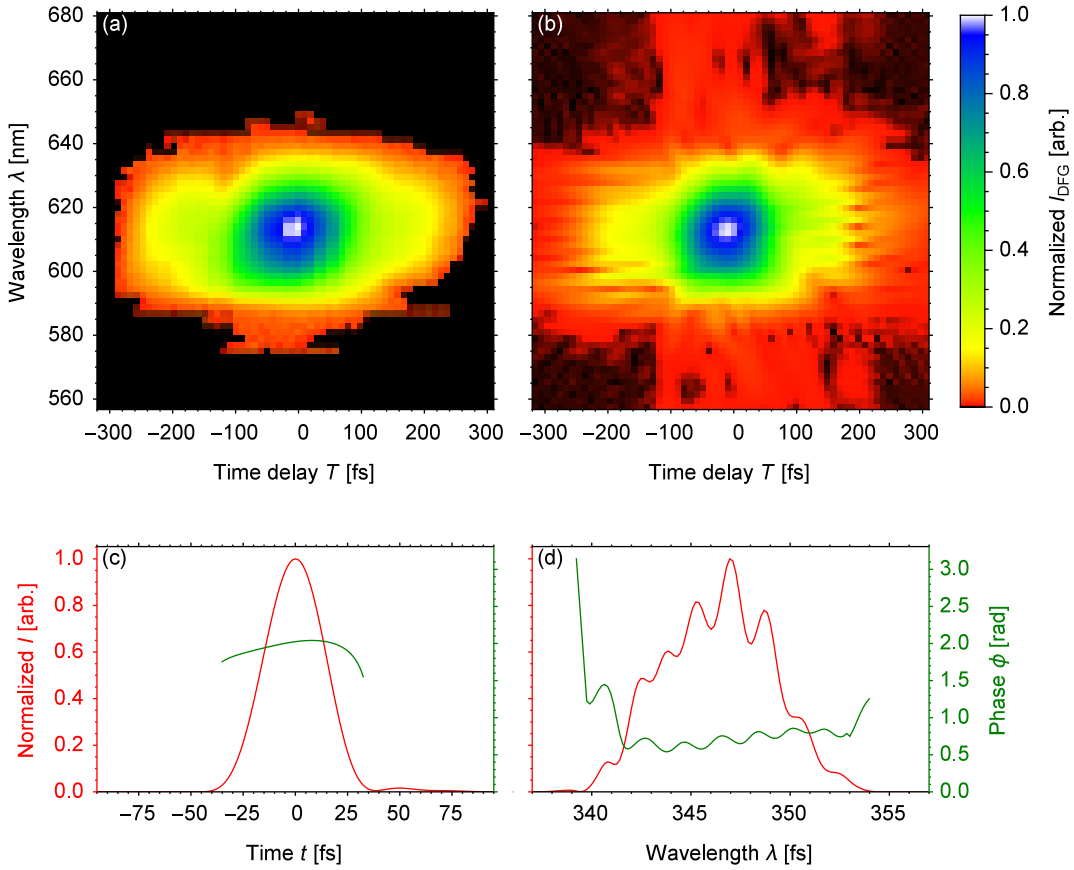

Fig. 1 Measured (a) and reconstructed (b) XFROG trace of the 348 nm pump pulse and the resulting temporal (c) and spectral (d) intensity (red) and phase (green). The XFROG error is 2.2 %, the temporal FWHM 34 fs and the FWHM bandwidth 6.2 nm.

[a] *Institut für Physikalische und Theoretische Chemie, Universität Würzburg, Am Hubland, D-97074 Würzburg, Germany; E-mail: brixner@phys-chemie.uni-wuerzburg.de*
[b] *J. Heyrovský Institute of Physical Chemistry v.v.i., Academy of Sciences of the Czech republic, Dolejškova 3, 182 23 Praha 8, Czech Republic*
[c] *Physikalische Chemie II, Ruhr-Universität Bochum, 44780 Bochum, Germany.*

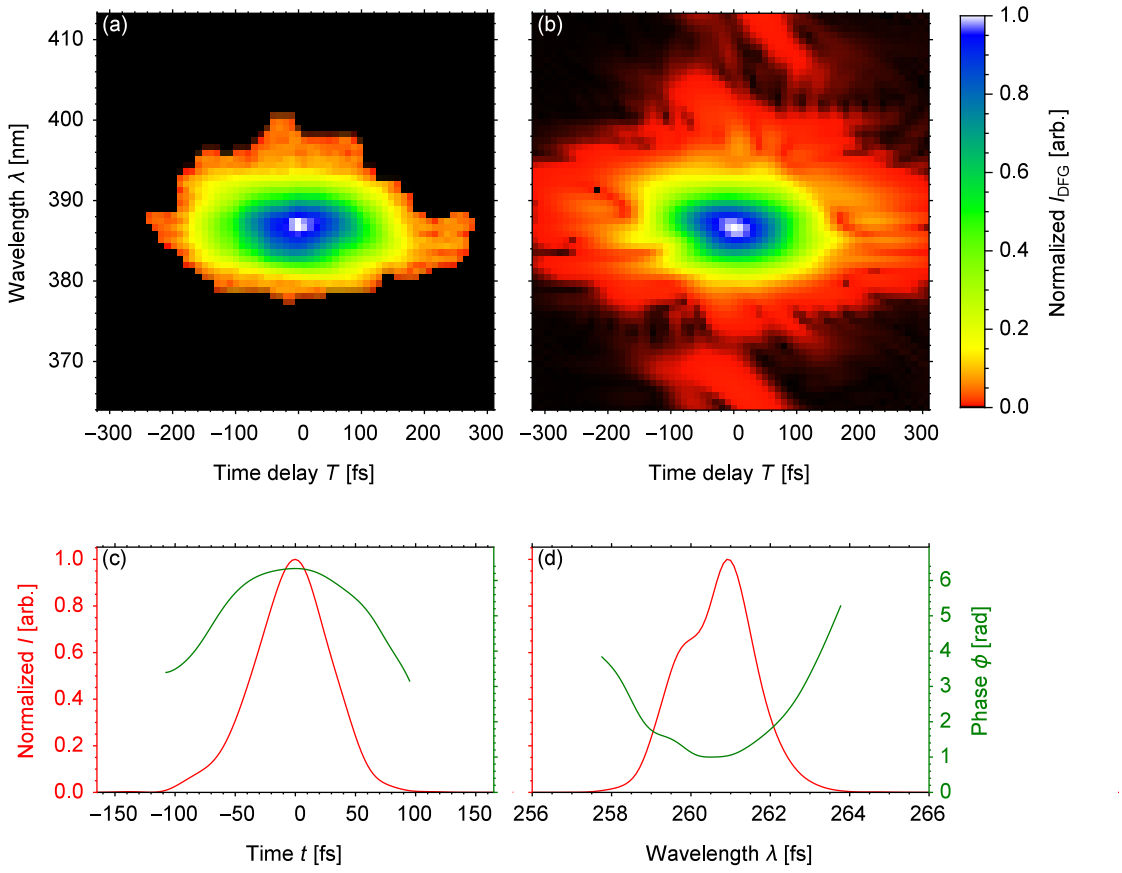

Fig. 2 Measured (a) and reconstructed (b) XFROG trace of the 261 nm pump pulse and the resulting temporal (c) and spectral (d) intensity (red) and phase (green). The XFROG error is 2.1 %, the temporal FWHM 72 fs and the FWHM bandwidth 2.3 nm.

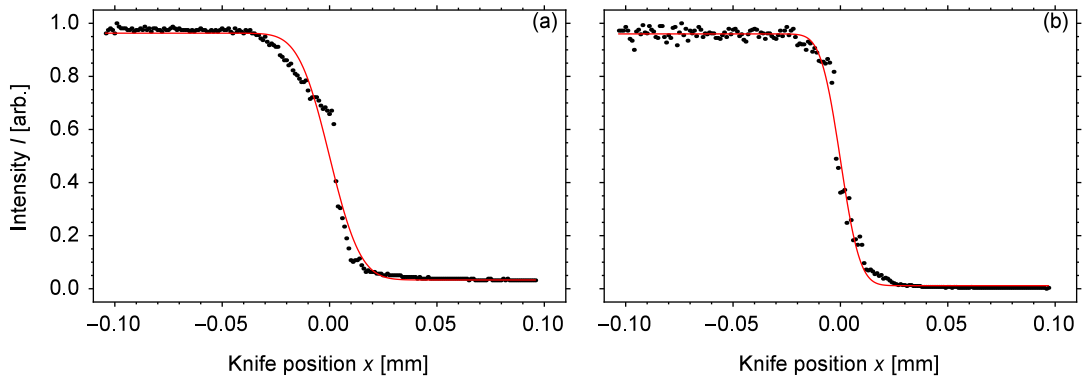

Fig. 3 Knife-edge scan of the 348 nm pump (a) and the (310-610) nm probe WL (b). The fitted error function (red) corresponds to a Gaussian with 27 μm spatial FWHM for the pump and 17 μm spatial FWHM for the probe.

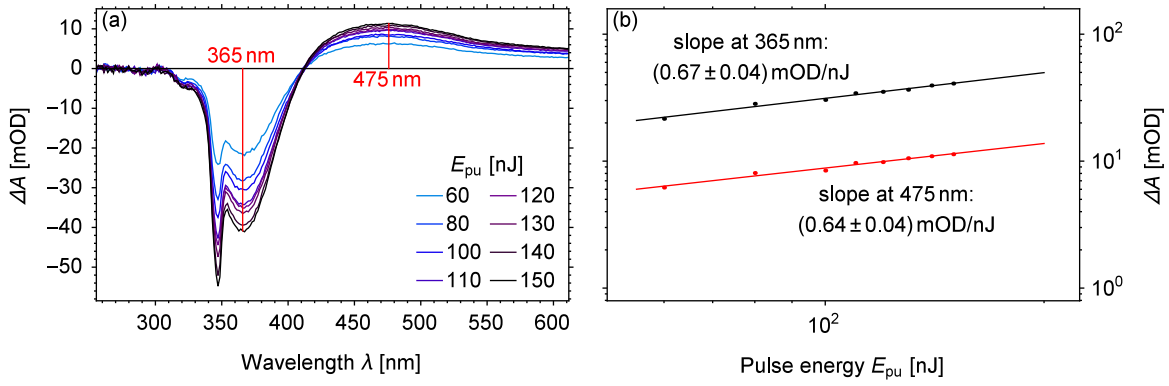

Fig. 4 Pump-energy dependency of the (310-610) nm difference spectrum at 3.34 ps for pumping at 348 nm (a) and the log–log slope at the GSB (365 nm) and at the PA (475 nm) (b). Since the slope is below one, the experiment is carried out in the saturation regime.

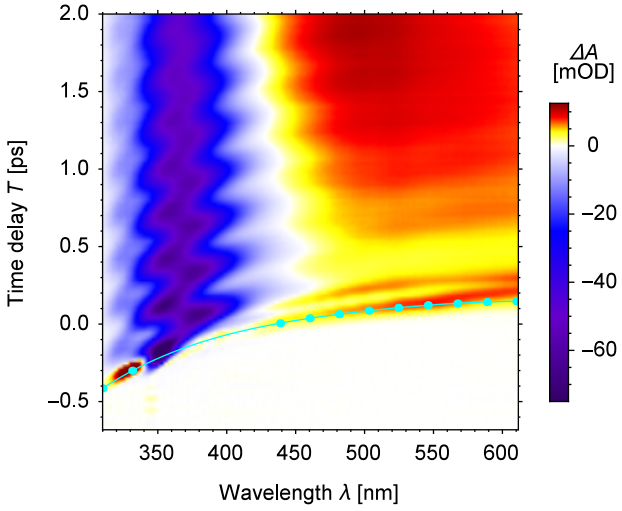

Fig. 5 Transient absorption spectrum of the I_3^- short-time dynamics in DCM after pumping at 348 nm. The pump stray light was removed and for the WL chirp correction a fourth-order polynomial (cyan curve) was fitted to manually selected t_0 points (cyan dots).

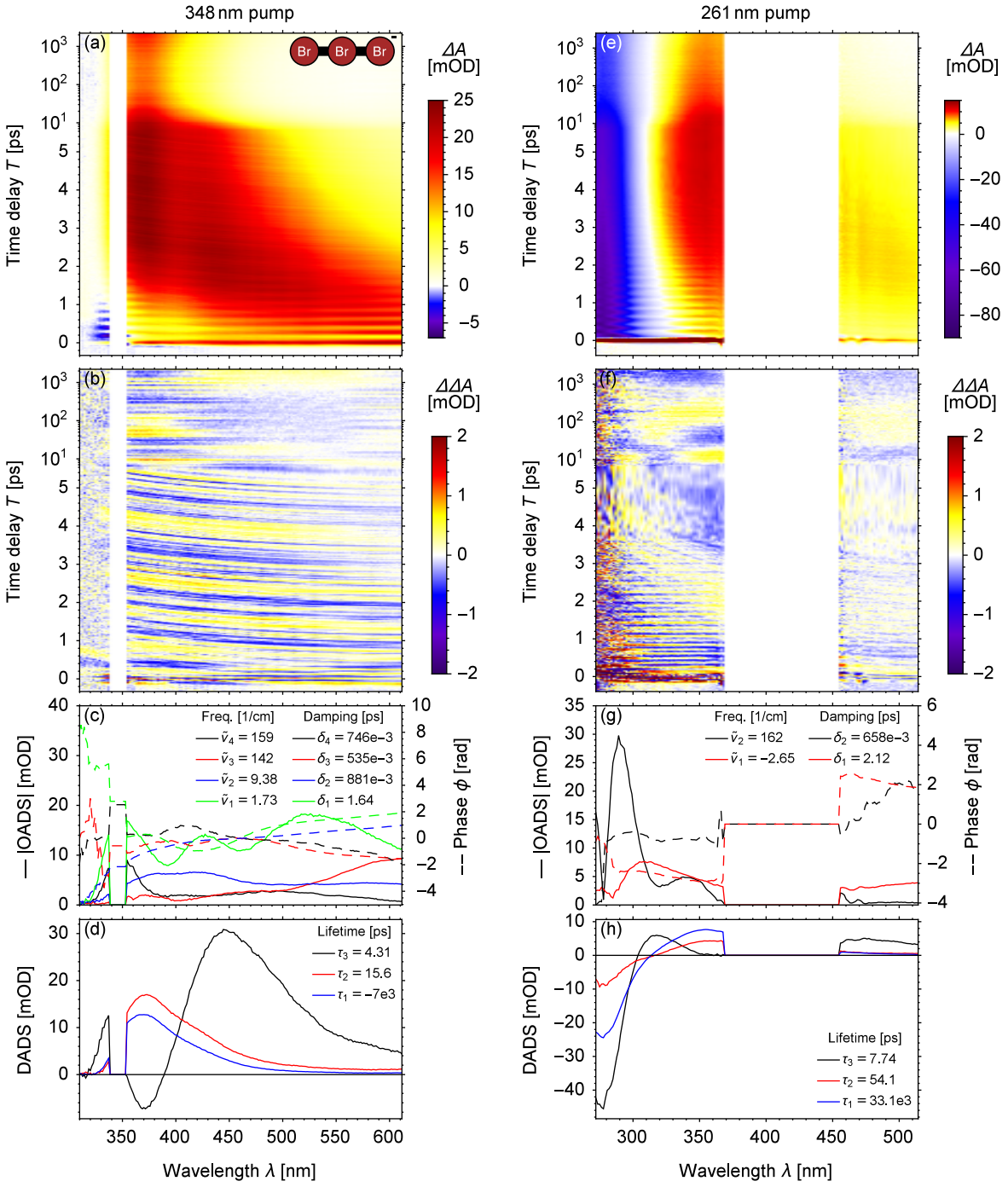

Fig. 6 Transient absorption data of Br_3^- pumped at 348 nm (a)-(d) and pumped at 261 nm (e)-(h). The transient absorption spectra (a), (e) were fitted similar to I_3^- in the main paper, where also the weak fragment oscillations of the fit residuals (b), (f) are discussed. Like for I_3^-, the main part of the Br_3^- model function consists of a combination of damped oscillations and decaying exponentials with the corresponding OADS (c), (g) and DADS (d), (h), respectively.

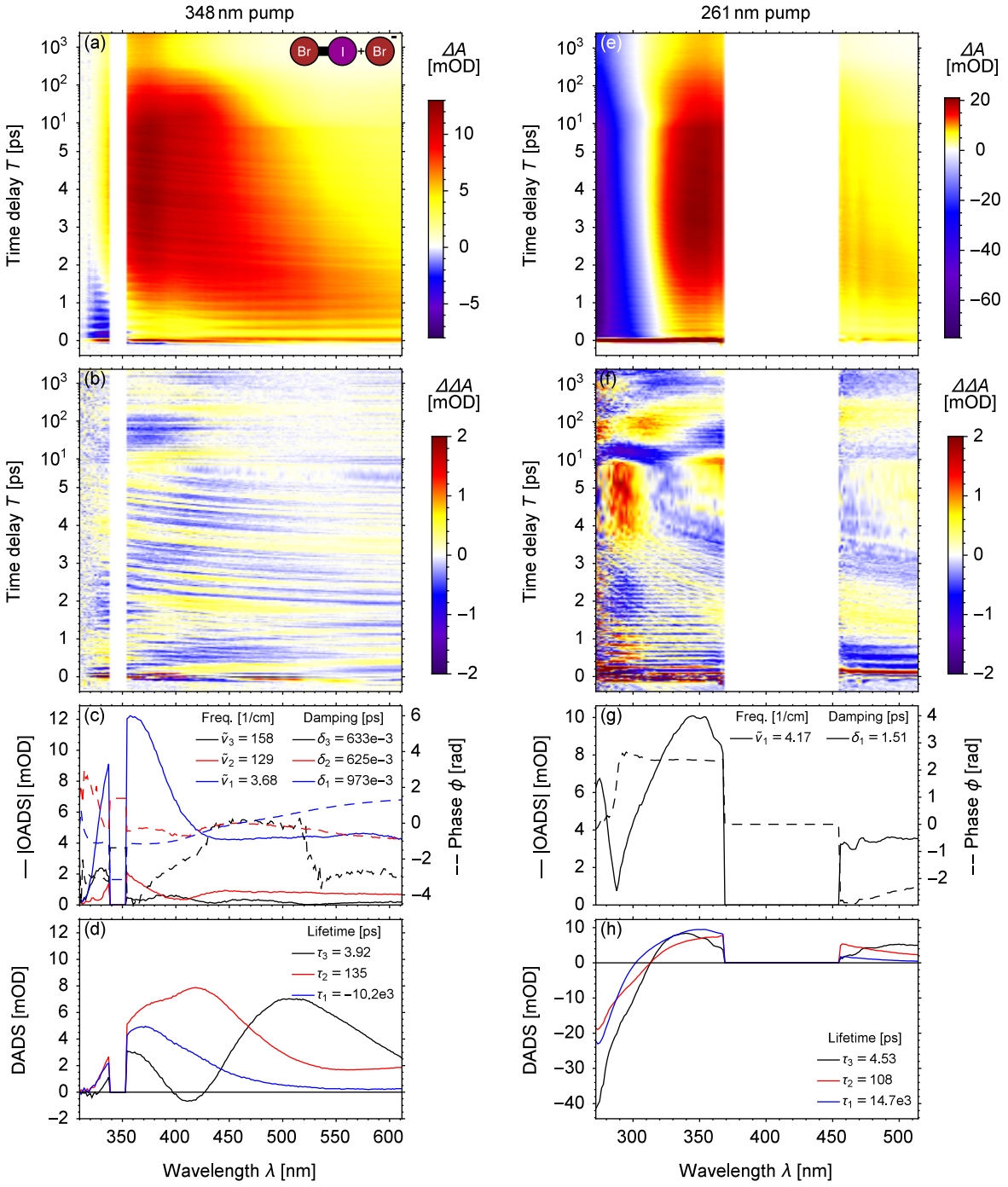

Fig. 7 Transient absorption data of the $IBr + Br^-$ sample pumped at 348 nm (a)-(d) and pumped at 261 nm (e)-(h). The transient absorption spectra (a), (e) were fitted similar to I_3^- in the main paper, where also the weak fragment oscillations of the fit residuals (b), (f) are discussed. Like for I_3^-, the main part of the IBr_2^- model function consists of a combination of damped oscillations and decaying exponentials with the corresponding OADS (c), (g) and DADS (d), (h), respectively.

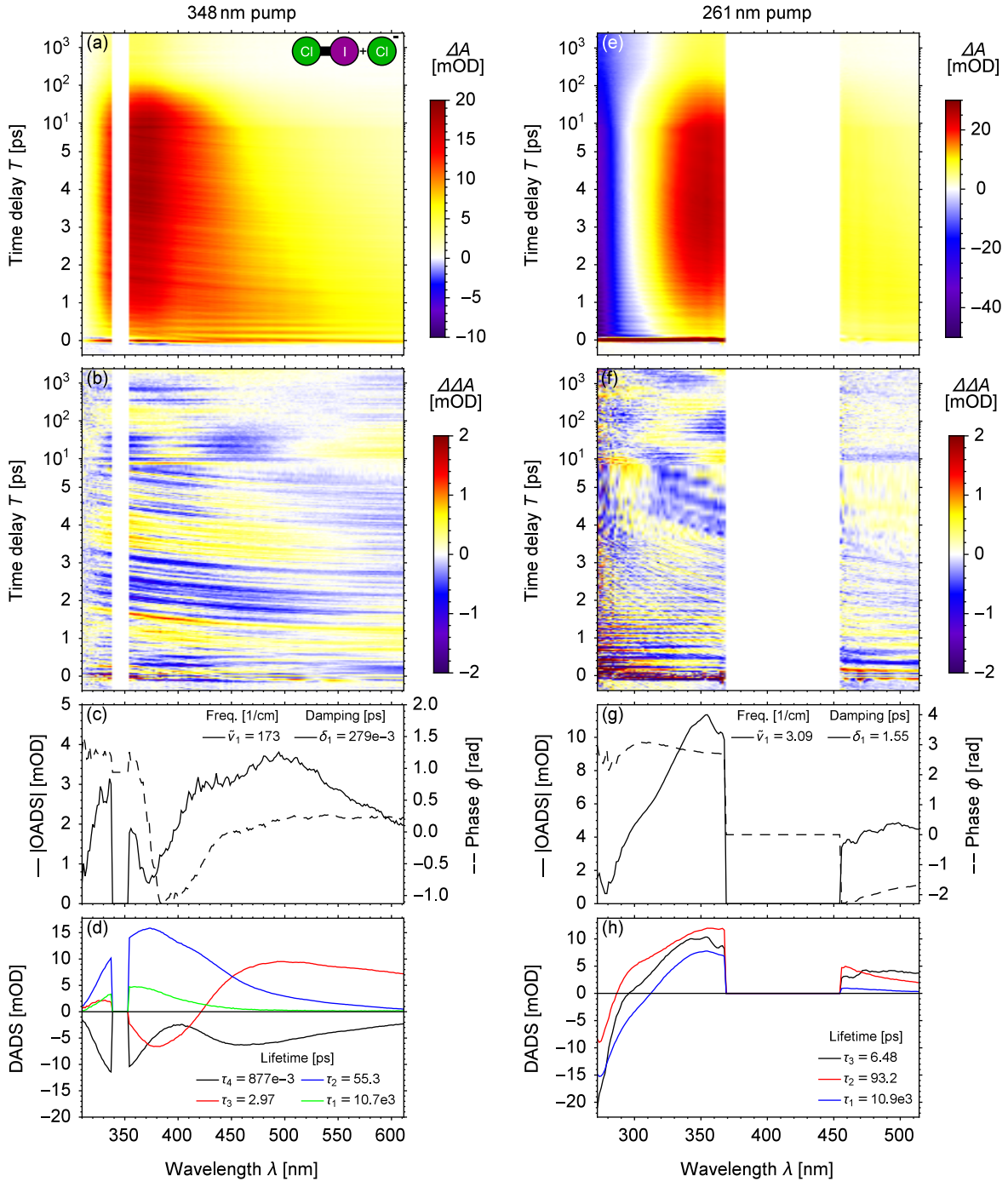

Fig. 8 Transient absorption data of the $ICl + Cl^-$ sample pumped at 348 nm (a)-(d) and pumped at 261 nm (e)-(h). The transient absorption spectra (a), (e) were fitted similar to I_3^- in the main paper, where also the weak fragment oscillations of the fit residuals (b), (f) are discussed. Like for I_3^-, the main part of the ICl_2^- or the ICl_2^-/I_2Cl^- model functions consists of a combination of damped oscillations and decaying exponentials with the corresponding OADS (c), (g) and DADS (d), (h), respectively.

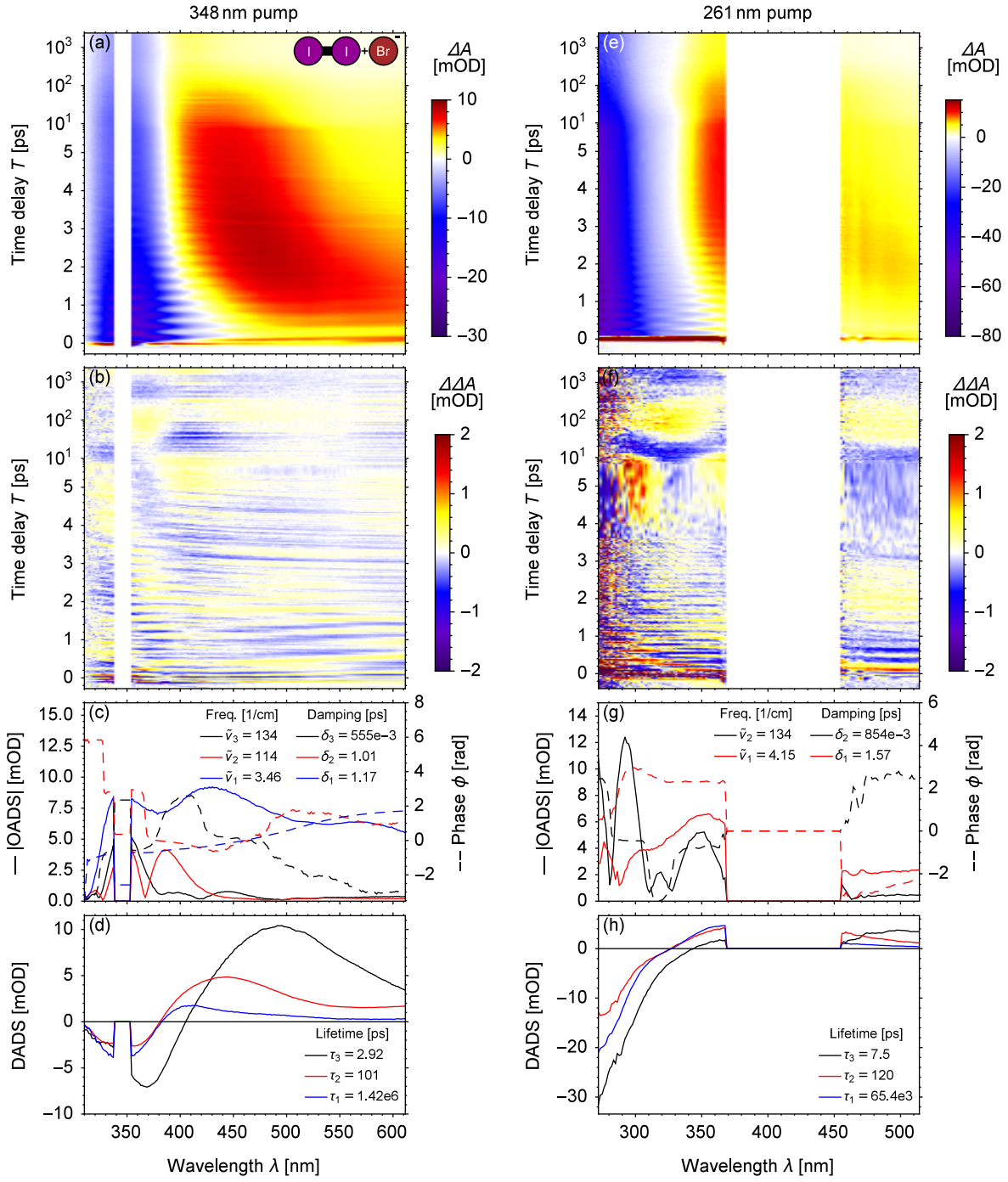

Fig. 9 Transient absorption data of $I_2 + Br^-$ pumped at 348 nm (a)-(d) and pumped at 261 nm (e)-(h). The transient absorption spectra (a), (e) were fitted similar to I_3^- in the main paper, where also the weak fragment oscillations of the fit residuals (b), (f) are discussed. Like for I_3^-, the main part of the I_3^-/I_2Br^- model functions consists of a combination of damped oscillations and decaying exponentials with the corresponding OADS (c), (g) and DADS (d), (h), respectively.

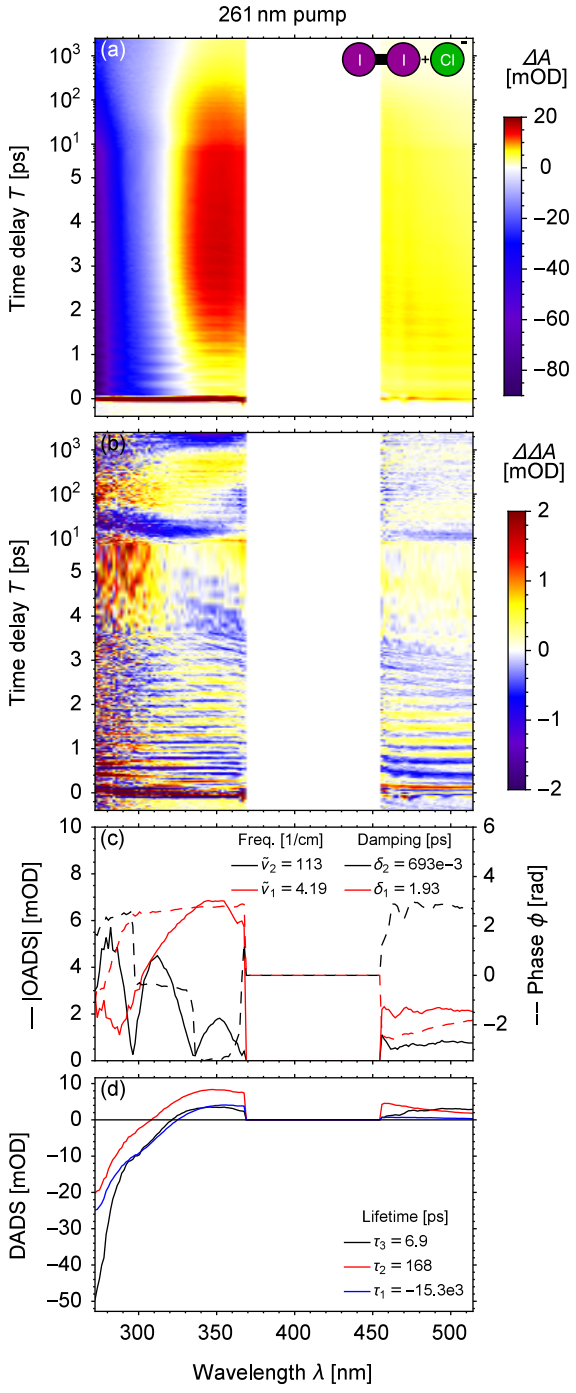

Fig. 10 Transient absorption data of $I_2 + Cl^-$ pumped at 261 nm. The transient absorption spectra (a) were fitted similar to I_3^- in the main paper, where also the weak fragment oscillations of the fit residuals (b) are discussed. Like for I_3^-, the main part of the I_3^-/I_2Cl^- model functions consists of a combination of damped oscillations and decaying exponentials with the corresponding OADS (c) and DADS (d), respectively.